PERGAMON

International Journal of Heat and Mass Transfer 45 (2002) 4217–4225

International Journal of HEAT and MASS TRANSFER

www.elsevier.com/locate/ijhmt

Laminar natural convection in differentially heated rectangular enclosures with vertical diffusive walls

V.A.F. Costa *

Departamento de Engenharia Mecânica, Universidade de Aveiro, Campus Universitário de Santiago, 3810-193 Aveiro, Portugal

Received 22 December 2000; received in revised form 28 September 2001

Abstract

Real enclosures have diffusive walls. A procedure is developed to evaluate the natural convection effective global Nusselt number for rectangular enclosures with vertical diffusive walls. The effective Nusselt number is evaluated using the temperature difference imposed over the exterior faces of the enclosure, the usual correlations for rectangular enclosures without diffusive walls, and the diffusive properties of the solid vertical walls, which are concentrated on a single dimensionless parameter. The proposed procedure is tested by comparing the obtained results with those achieved from the complete two-dimensional numerical simulation of the conjugated heat transfer problem occurring in the complete enclosure, with diffusive walls. The result is a helpful tool that promptly helps the thermal engineer when dealing with enclosures with diffusive walls.

1. Introduction

Laminar natural convection in differentially heated rectangular enclosures is one of the most extensively studied problems in numerical and experimental terms [1–4]. There are well-established correlations available to evaluate the Nusselt number corresponding to such enclosures [1,3], as well as bench-mark numerical solutions for this problem [2]. However, the usual situations analyzed refer to rectangular enclosures without vertical diffusive walls, with imposed uniform temperatures at the vertical surfaces, and with perfectly insulated upper and lower walls.

It is well known that such enclosures do not appear in real case scenarios. A closest situation to reality is the enclosure with diffusive vertical walls and adiabatic upper and lower walls. The analysis of the natural convection problem in rectangular enclosures with diffusive walls has been object of previous work [5–13], but further work is required in what concerns design and development. At present, there is no work that promptly helps the thermal engineer when dealing with such real enclosures. It is expected, from an engineering point of view, the evaluation of the effective Nusselt number for enclosures with diffusive walls, in a way similar to that followed when dealing with enclosures without diffusive walls (or with walls of very high thermal diffusivities).

This work aims to develop and test a procedure to promptly help the thermal engineer when evaluating the effective Nusselt number corresponding to rectangular enclosures with diffusive vertical walls. In fact, the latter is believed to incorporate conditions enabling a better description of the real enclosures. Once known the imposed temperatures at the exterior faces of the complete enclosure with diffusive walls, and the usual correlations for the global Nusselt number in rectangular enclosures without diffusive walls, one can obtain a global Nusselt number that is not the effective global Nusselt number. The thermal properties of the diffusive walls can be concentrated on a single dimensionless parameter, the explained procedure acting like a correction over the so-obtained global Nusselt number in order to obtain the effective global Nusselt number.

The developed procedure is based on a one-dimensional (1D) approach, which is only a simplified model of the two-dimensional (2D) problem. In order to assess the validity of such methodology, the results obtained with the 1D approach are extensively compared with the

* Tel.: +351-234-370-829; fax: +351-234-370-953.
E-mail address: v_costa@mec.ua.pt (V.A.F. Costa).

0017-9310/02/$ - see front matter
PII: S0017-9310(02)00125-4

Nomenclature

B	wall thickness
C	constant (in the correlation)
F	dimensionless factor
g	gravitational acceleration
H	height
k	thermal conductivity
L	horizontal length
$\overline{Nu}$	average Nusselt number
n_1, n_2	constants (in the correlation)
p	pressure
Pr	Prandtl number
$\dot{Q}'$	heat flow, by unit depth
Ra	Rayleigh number
T	temperature
u, v	Cartesian velocity components
x, y	Cartesian co-ordinates

Greek symbols

α	thermal diffusivity
β	volumetric expansion coefficient
v	kinematic viscosity
ρ	density

Subscripts

f	fluid medium
H	based on the H height
s	solid medium
y	at the level y
1,2,3,4	vertical surfaces
*	dimensionless

Superscript

0	based on the $T_1 - T_4$ temperature difference

2D ones, obtained from the complete numerical simulation of the conjugated heat transfer problem taking place in the complete enclosure with diffusive walls. The results obtained clearly highlight the validity of the proposed procedure to evaluate the effective Nusselt number. Nevertheless, special conditions that may lead to deviations are pointed and discussed.

2. Physical model and assumptions

The situation under consideration is presented in Fig. 1, where the vertical walls of thickness B are heat diffusive, with thermal conductivity k_s. The hot and cold temperatures are imposed over the extreme dimensions of the enclosure, i.e. over the external surfaces of the diffusive lateral walls of the enclosure. It will be assumed that the hot wall is the left one, with a temperature T_1, and that the cold wall is the right wall, with a temperature T_4. The upper and lower walls are assumed to be perfectly insulated.

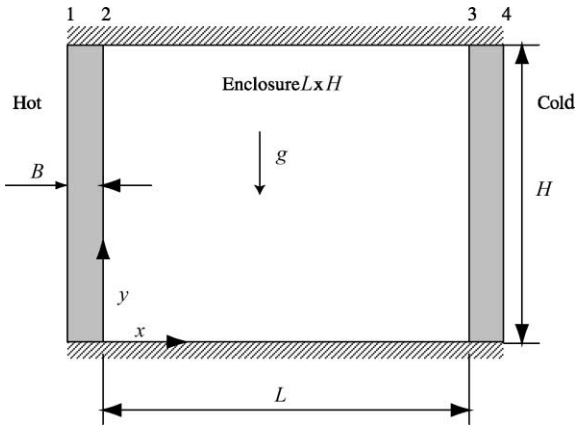

Fig. 1. Physical model and geometry.

The enclosure is filled with a Newton–Fourier fluid, which is incompressible but expands or contracts with temperature changes. This assumption leads to the use of the Boussinesq approximation in the vertical momentum source term, if the maximum temperature difference (in the fluid) is maintained low [1]. It is assumed that the hot and cold thermal levels are small and similar enough in order to neglect the thermal radiation transfer between the interior faces of the enclosure, and that the fluid is radiatively non-participating. The energy generation term due to viscous dissipation, and the change of temperature due to reversible deformation (work of pressure forces) are neglected. All the thermophysical properties of the involved media are assumed to be constant, exception made to the density appearing in the buoyancy term, which is treated as varying linearly with temperature. It is assumed that the flow field within the enclosure occurs only in the laminar regime, implying an enclosure Rayleigh number lower than $\approx 10^8$ [1].

Temperatures T_2 and T_3 are assumed to be nearly constant, i.e. it is assumed that the heat flow is 1D through the solid walls. This assumption will be discussed further.

3. One-dimensional model

3.1. Modeling

The actually recommended correlation for the laminar natural convection global Nusselt number of rect-

angular enclosures, with an aspect ratio near unit, is that proposed by Berkovsky and Polevikov [1,3] which is

$$\overline{Nu}_H = C\left(\frac{Pr}{0.2+Pr}Ra_H\right)^{n_1}\left(\frac{L}{H}\right)^{n_2} \tag{1}$$

when the Rayleigh number is based on height H. The involved constants and applicability conditions of this correlation are given in Table 1. In the present case, constant C (in the second row of Table 1) was slightly modified ($C = 0.17$) in order to obtain a better correlation for Nusselt numbers achieved using the complete 2D model. In fact, correlation (1) with $C = 0.18$ gives Nusselt numbers somewhat high even when compared with the ones taken from the bench-mark numerical solution [2].

Once known the temperatures imposed at the exterior faces of the complete enclosure, it can be evaluated the and H based Rayleigh number

$$Ra_H^0 = \frac{g\beta(T_1 - T_4)H^3}{\nu\alpha} \tag{2}$$

From correlation (1) it can be obtained the global Nusselt number $\overline{Nu}_H^0$, using the Ra_H^0 Rayleigh number. The heat transferred through the enclosure without diffusive walls is thus $\dot{Q}'^0 = [k_f H(T_1 - T_4)/L]\overline{Nu}_H^0$. However, the effective temperature difference felt by the fluid within the enclosure is not $T_1 - T_4$ but $T_2 - T_3$, assuming that T_2 and T_3 are nearly constant. Therefore, the $T_2 - T_3$ and H based effective Rayleigh number can be obtained as $Ra_H = g\beta(T_2 - T_3)H^3/(\nu\alpha)$. In this case, the effective heat transferred through the enclosure with diffusive walls is $\dot{Q}' = [k_f H(T_2 - T_3)/L]\overline{Nu}_H$. From correlation (1) it can be also obtained the effective global Nusselt number, $\overline{Nu}_H$, using the effective Rayleigh number, Ra_H.

If the applicability conditions and the used correlation are kept unchanged for both $\overline{Nu}_H^0$ and $\overline{Nu}_H$, it can be obtained that

$$\frac{\overline{Nu}_H}{\overline{Nu}_H^0} = \left(\frac{Ra_H}{Ra_H^0}\right)^{n_1} \tag{3}$$

Once known the ratio Ra_H/Ra_H^0, the global effective Nusselt number $\overline{Nu}_H$ can be evaluated, since the global Nusselt number $\overline{Nu}_H^0$ is readily known from Eqs. (1) and (2). However, it remains to be evaluated the temperature difference $T_2 - T_3$.

Attempting on Fig. 1, from the 1D approach, it can be obtained that

$$\dot{Q}' = k_s H\frac{T_1 - T_2}{B} \Rightarrow T_1 - T_2 = \dot{Q}'\frac{B}{k_s H} \tag{4a}$$

$$\dot{Q}' = k_f H\frac{T_2 - T_3}{L}\overline{Nu}_H \Rightarrow T_2 - T_3 = \dot{Q}'\frac{L}{k_f H}\frac{1}{\overline{Nu}_H} \tag{4b}$$

$$\dot{Q}' = k_s H\frac{T_3 - T_4}{B} \Rightarrow T_3 - T_4 = \dot{Q}'\frac{B}{k_s H} \tag{4c}$$

results that can be added and arranged to give

$$\dot{Q}' = k_f H\frac{T_1 - T_4}{L}\frac{\overline{Nu}_H}{F\overline{Nu}_H + 1} \tag{5}$$

where

$$F \equiv 2\frac{B}{L}\frac{k_f}{k_s} \tag{6}$$

F is therefore a dimensionless parameter concentrating the diffusive properties of the vertical diffusive walls. This factor can be interpreted as $F \equiv (2B/k_s)/(L/k_f)$, i.e. the ratio between the diffusive resistances of the solid walls and of the enclosure filling fluid.

The global Nusselt number for enclosures is defined as the ratio of the global heat flow effectively transferred due to convection and the global heat flow transferred by pure conduction only through the stagnant fluid. This definition of the Nusselt number is present in Eq. (4b). In the present case, the natural convection problem lies in the definition of the temperature difference between the interior faces of the enclosure, which is the maximum temperature difference experienced by the fluid.

The effective temperature difference $T_2 - T_3$ experienced by the enclosure filling fluid is obtained from Eqs. (4b) and (5) as

$$\frac{T_2 - T_3}{T_1 - T_4} = T_{2^*} - T_{3^*} = \frac{Ra_H}{Ra_H^0} = \frac{1}{F\overline{Nu}_H + 1} \tag{7}$$

the temperature being made dimensionless through

$$T_* = \frac{T - T_4}{T_1 - T_4} \tag{8}$$

Combining Eq. (7) into Eq. (3) it can be obtained that

$$\frac{\overline{Nu}_H}{\overline{Nu}_H^0} = \left(F\overline{Nu}_H + 1\right)^{-n_1} \tag{9}$$

Thus, once known the $T_1 - T_4$ based Nusselt number $\overline{Nu}_H^0$ and the F factor, the effective Nusselt number $\overline{Nu}_H$,

Table 1
Applicability conditions and constants of the Berkovsky and Polevikov correlation [3]

L/H	Pr	Ra_H	C	n_1	n_2
$0.1 < L/H < 0.5$	$Pr < 10^5$	$Ra_H < 10^{13}$	0.22	0.28	0.09
$0.5 < L/H < 1.0$	$10^{-3} < Pr < 10^5$	$[Pr/(0.2+Pr)]Ra_H(L/H)^3 > 10^3$	0.18	0.29	−0.13

based on the $T_2 - T_3$ temperature difference, can be obtained from the non-linear equation (9). Once known the $\overline{Nu}_H$ Nusselt number, the $T_2 - T_3$ temperature difference can be obtained from Eq. (7).

The ratio $\dot{Q}'/\dot{Q}'^{,0}$ between the effective heat transfer rate and the heat transfer rate corresponding to the enclosure without diffusive walls, both per unit depth, can be obtained as

$$\frac{\dot{Q}'}{\dot{Q}'^{0}} = \frac{k_f H \frac{T_1 - T_4}{L} \frac{\overline{Nu}_H}{F\overline{Nu}_H + 1}}{k_f H \frac{T_1 - T_4}{L} \overline{Nu}_H^0} = \left(F\overline{Nu}_H + 1\right)^{-(n_1+1)} \tag{10}$$

The following limit situations of Eqs. (7), (9) and (10) can be referred:

$$T_{2^*} - T_{3^*} \to 1, \quad \overline{Nu}_H/\overline{Nu}_H^0 \to 1, \quad \dot{Q}'/\dot{Q}'^0 \to 1 \quad \text{if } F \to 0 \tag{11a}$$

and

$$T_{2^*} - T_{3^*} \to 0, \quad \overline{Nu}_H/\overline{Nu}_H^0 \to 0, \quad \dot{Q}'/\dot{Q}'^0 \to 0 \quad \text{if } F \to +\infty \tag{11b}$$

$F \to 0$ corresponds to walls with high thermal conductivity or very thin walls, thus corresponding to a situation similar to the rectangular enclosure without diffusive walls, in terms of temperature distribution and effective global Nusselt number. $F \to +\infty$ corresponds to walls of very low thermal conductivity or very thick walls, the main temperature differences occurring through the diffusive walls which act as insulators, and the temperature is essentially constant through the fluid within the enclosure. Thus, when F is moderate or large, an enclosure with diffusive walls is strongly different from the one without diffusive walls in terms of temperature distribution, the effective global Nusselt number and the heat effectively transferred.

The $\overline{Nu}_H/\overline{Nu}_H^0$ ratio obtained from Eq. (9) is depicted in Fig. 2 as a function of the $\overline{Nu}_H^0$ Nusselt number and of the F factor, using the data of the second row of Table 1 in correlation (1), with $C = 0.17$. This same correlation and set of values will be used in what follows. It can be observed that $\overline{Nu}_H \approx \overline{Nu}_H^0$ for small values of the F factor, and $\overline{Nu}_H < \overline{Nu}_H^0$ for moderate and high values of the F factor, i.e. the ratio $\overline{Nu}_H/\overline{Nu}_H^0$ decreases as F increases. It is thus observed that the effective Nusselt number is affected (or even severely affected) by the presence of diffusive walls.

Some results obtained from Eq. (7) are depicted in Fig. 3, where the dimensionless temperature difference $T_{2^*} - T_{3^*}$ is a function of the $\overline{Nu}_H^0$ Nusselt number and of the F factor. It is observed that $T_{2^*} - T_{3^*} \approx 1$ for small values of the F factor, and that $T_{2^*} - T_{3^*} < 1$ for moderate or high values of the F factor, i.e. the dimensionless temperature difference $T_{2^*} - T_{3^*}$ decreases as F increases. It can also be observed that the effective temperature

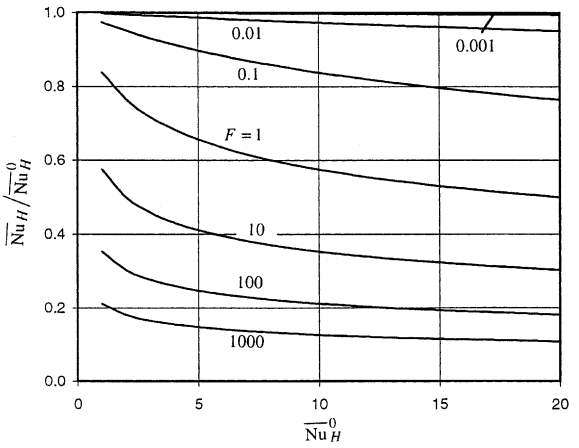

Fig. 2. The ratio $\overline{Nu}_H/\overline{Nu}_H^0$, obtained from the 1D modeling, as function of the $\overline{Nu}_H^0$ Nusselt number for some values of the F factor.

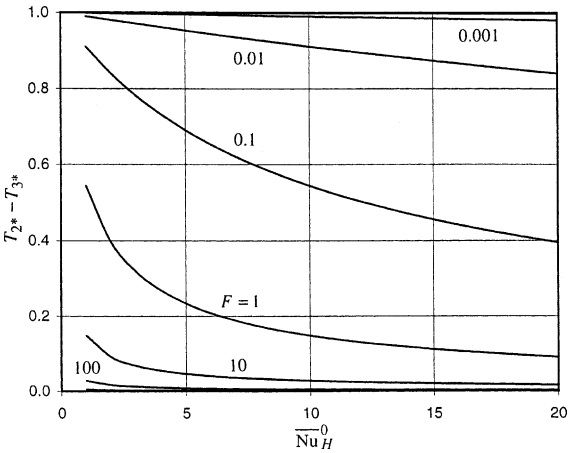

Fig. 3. The dimensionless effective temperature difference $(T_2 - T_3)/(T_1 - T_4)$ experienced by the fluid within the enclosure, obtained from the 1D modeling, as function of the $\overline{Nu}_H^0$ Nusselt number for some values of the F factor.

difference experienced by the fluid within the enclosure is strongly affected by the diffusive walls for moderate and high values of F.

The $\dot{Q}'/\dot{Q}'^0$ ratio obtained from Eq. (10) is depicted in Fig. 4, as a function of the $\overline{Nu}_H^0$ Nusselt number and of the F factor. It is observed that $\dot{Q}'/\dot{Q}'^0 \approx 1$ for small values of the F factor, and that $\dot{Q}'/\dot{Q}'^0 < 1$ for moderate and high values of the F factor, the ratio $\dot{Q}'/\dot{Q}'^0$ decreasing as F increases. It is also observed that the global effective heat transfer rate through the complete enclosure is also severely affected by the presence of the diffusive walls for moderate and high values of F.

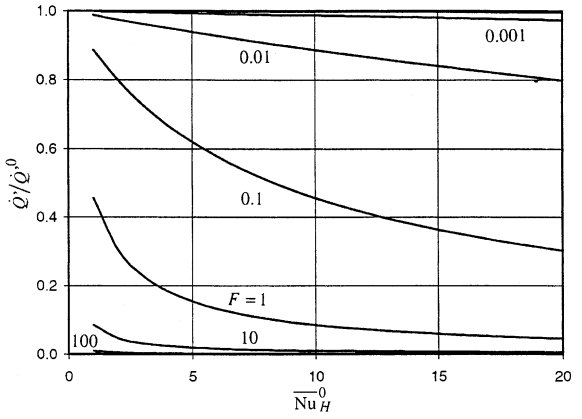

Fig. 4. The ratio $\dot{Q}'/\dot{Q}'^0$, obtained from the 1D modeling, as function of the $\overline{Nu}_H^0$ Nusselt number for some values of the F factor.

3.2. Discussion

The foregoing 1D model is an extremely useful way to evaluate the effective Nusselt number, the effective temperature difference and the effective heat flow transferred through the complete enclosure with diffusive walls, once known the temperature difference $T_1 - T_4$, the F factor and the applicable correlation for the Nusselt number. The Nusselt number $\overline{Nu}_H^0$ is easily calculated from the already known temperature difference $T_1 - T_4$. The effective Nusselt number, $\overline{Nu}_H$, is based on the a priori unknown maximum temperature difference experienced by the fluid within the enclosure, $T_2 - T_3$. The main goal of this work is to obtain the effective global Nusselt number $\overline{Nu}_H$ from the easy to calculate $\overline{Nu}_H^0$ Nusselt number. It remains to be evaluated if this 1D approach is correct enough to be used for calculation purposes. The main source of uncertainty lies on the assumed uniform temperatures at the interior faces of the enclosure and on the 1D model used. In order to evaluate the applicability of the procedure, one needs to solve the complete 2D problem and compare the results. The solution of the 2D problem needs to be solved numerically, as explained in Section 4.

It should be noted that the ratio L/H is not relevant to evaluate the validity of the proposed 1D procedure, and that the main governing parameter is solely the F factor. Thus, tests will be conducted for a quadrangular enclosure $(L/H = 1)$ with diffusive walls, for different values of the F factor. It remains to be analyzed how the factor F acts over the temperature distributions along the vertical solid–fluid interfaces of the enclosure, over the effective Nusselt number and over the heat effectively transferred, for several values of other governing dimensionless parameters such as the Prandtl and Rayleigh numbers.

4. Two-dimensional model

4.1. Modeling

The complete problem under consideration is governed by the 2D mass, momentum and energy conservation equations in the fluid domain, which are, in the conservative non-dimensional form, respectively,

$$\frac{\partial u_*}{\partial x_*} + \frac{\partial v_*}{\partial y_*} = 0 \tag{12}$$

$$\frac{\partial}{\partial x_*}(u_* u_*) + \frac{\partial}{\partial y_*}(v_* u_*) = -\frac{\partial p_*}{\partial x_*} + Pr\left(\frac{\partial^2 u_*}{\partial x_*^2} + \frac{\partial^2 u_*}{\partial y_*^2}\right) \tag{13}$$

$$\frac{\partial}{\partial x_*}(u_* v_*) + \frac{\partial}{\partial y_*}(v_* v_*) = -\frac{\partial p_*}{\partial y_*} + Pr\left(\frac{\partial^2 v_*}{\partial x_*^2} + \frac{\partial^2 v_*}{\partial y_*^2}\right) + Ra_H^0 Pr T_* \tag{14}$$

$$\frac{\partial}{\partial x_*}(u_* T_*) + \frac{\partial}{\partial y_*}(v_* T_*) = \frac{\partial^2 T_*}{\partial x_*^2} + \frac{\partial^2 T_*}{\partial y_*^2} \tag{15}$$

and by the energy conservation equation in the solid vertical walls

$$0 = \frac{\partial^2 T_*}{\partial x_*^2} + \frac{\partial^2 T_*}{\partial y_*^2} \tag{16}$$

The original mass, momentum and energy conservation equations were made dimensionless through the introduction of the non-dimensional variables

$$x_* = x/H; \quad y_* = y/H \tag{17}$$

$$u_* = \frac{u}{\alpha/H}; \quad v_* = \frac{v}{\alpha/H} \tag{18}$$

$$p_* = \frac{p + \rho_4 g y}{\rho_4 (\alpha/H)^2} \tag{19}$$

The temperature is made dimensionless as given by Eq. (8), and the Ra_H^0 Rayleigh number is obtained from Eq. (2).

4.2. Boundary conditions

The boundary conditions for the foregoing differential equations are:

Over the solid walls, $u_* = v_* = 0$.

Imposed temperatures at the exterior faces of the solid walls

$$T_*(-B_*, y_*) = 1; \quad T_*(L_* + B_*, y_*) = 0 \tag{20}$$

Perfect insulation at the upper and lower faces of the enclosure

$$(\partial T_*/\partial y_*)_{(x_*,0)} = (\partial T_*/\partial y_*)_{(x_*,1)} = 0 \tag{21}$$

Continuity of the heat flux at the solid–fluid interfaces

$$\left(\frac{\partial T_*}{\partial x_*}\right)_{\mathrm{f}} = \frac{k_{\mathrm{s}}}{k_{\mathrm{f}}}\left(\frac{\partial T_*}{\partial x_*}\right)_{\mathrm{s}}(0,y_*) \quad \text{and} \quad (L_*,y_*) \tag{22}$$

Continuity of the temperature at the solid–fluid interfaces

$$(T_*)_{\mathrm{f}} = (T_*)_{\mathrm{s}}(0,y_*) \quad \text{and} \quad (L_*,y_*) \tag{23}$$

4.3. Heat transfer rate

The local heat transfer rate occurring between the hot and cold walls can be evaluated at any convenient constant x surface. For convenience, it can be evaluated at the fluid side of the solid–fluid interface located at $x_* = 0$, where the velocity is null, the global heat transfer rate (by unit depth) through the complete enclosure being obtained as

$$\dot{Q}' = \int_0^H \left(-k_{\mathrm{f}}\frac{\partial T}{\partial x}\right)_y \mathrm{d}y \tag{24}$$

Once known the temperature field T^0 from the 2D numerical simulation, for the enclosure without diffusive walls ($F \to 0$), the global Nusselt number $\overline{Nu}_H^0$ is evaluated as

$$\overline{Nu}_H^0 = \frac{\int_0^H \left(-k_{\mathrm{f}}\frac{\partial T^0}{\partial x}\right)_{x=0}\mathrm{d}y}{k_{\mathrm{f}}H(T_1-T_4)/L} = L_*\int_0^1 \left(-\frac{\partial T_*^0}{\partial x_*}\right)_{x_*=0}\mathrm{d}y_* \tag{25}$$

where superscript 0 means that the temperature difference $T_1 - T_4$ is felt by the fluid that fills the enclosure without diffusive walls. From the knowledge of the temperature field T, obtained from the 2D numerical simulation for the enclosure with diffusive walls, the effective global Nusselt number $\overline{\mathrm{Nu}}_H$ is evaluated as

$$\overline{Nu}_H = \frac{\int_0^H \left(-k_{\mathrm{f}}\frac{\partial T}{\partial x}\right)_{x=0}\mathrm{d}y}{k_{\mathrm{f}}H(T_2-T_3)/L} = \frac{L_*}{T_{2*}-T_{3*}}\int_0^1 \left(-\frac{\partial T_*}{\partial x_*}\right)_{x_*=0}\mathrm{d}y_* \tag{26}$$

In this equation, T_{2*} and T_{3*} are the average dimensionless temperatures over the $x_* = 0$ and $x_* = L_*$ vertical surfaces, respectively, obtained as

$$T_{2^*} = \int_0^1 (T_*)_{x_*=0}\mathrm{d}y_* \quad T_{3^*} = \int_0^1 (T_*)_{x_*=L_*}\mathrm{d}y_* \tag{27}$$

The ratio $\overline{Nu}_H/\overline{Nu}_H^0$ can be obtained from Eqs. (25) and (26).

The ratio $\dot{Q}'/\dot{Q}'^0$ between the effective heat transfer rate and the heat transfer rate corresponding to the enclosure without diffusive walls, both by unit depth, can be obtained from

$$\frac{\dot{Q}'}{\dot{Q}'^0} = \frac{[k_{\mathrm{f}}H(T_2-T_3)/L]\overline{Nu}_H}{[k_{\mathrm{f}}H(T_1-T_4)/L]\overline{Nu}_H^0} = \frac{\overline{Nu}_H}{\overline{Nu}_H^0}(T_{2^*}-T_{3^*}) \tag{28}$$

4.4. Numerical modeling

The 2D problem set by the system of differential equations (12)–(16), subject to the boundary conditions specified by Eqs. (20)–(23), is solved numerically using the control volume finite difference method, with staggered grids for the velocity components and the power-law scheme for the integration of the convection–diffusion terms [14]. The pressure–velocity link is established through the SIMPLER algorithm [14]. Over the fluid–solid interfaces, the conjugated heat and mass transfer problem is solved through the use of the harmonic mean practice for the diffusion coefficients [14,15], automatically imposing the continuity of the dependent variables at the interfaces. The discretization equations, formally the same for all variables, are solved iteratively with the TDMA algorithm applied several times (typically twice for all the variables other than the pressure, and five times for the pressure as well as for the pressure corrections) over a complete line in each co-ordinate direction.

The domain is descretized using a 65×57 non-uniform grid, symmetric relatively to the center of the enclosure in both x_* and y_* co-ordinate directions, expanding from the wall to the center with an expansion factor of 1.08. Four columns of nodes are considered over each vertical diffusive wall. This grid was selected after some preliminary tests of asymptotic type were carried out.

5. Results and comparison

The 1D procedure proposed is tested using a quadrangular enclosure filled with air ($Pr = 0.73$), for several values of the F factor and Ra_H^0 global Rayleigh number. The Berkovsky and Polevikov correlation (1) is used at the top border line $L/H = 1$. To the results obtained with the 1D procedure it has been assigned the 1D subscript, and to those obtained from the complete 2D modeling the 2D subscript. To assess the accuracy of the 1D procedure, the effective Nusselt number $\overline{Nu}_H$, the dimensionless effective temperature difference $T_{2^*} - T_{3^*}$ and the effective heat transferred $\dot{Q}'$ obtained from the complete 2D modeling will be taken as the effective reference values.

In Fig. 5 it is presented the ratio $\left(\overline{Nu}_H/\overline{Nu}_H^0\right)_{2\mathrm{D}}/\left(\overline{Nu}_H/\overline{Nu}_H^0\right)_{1\mathrm{D}}$ as function of the F factor for different

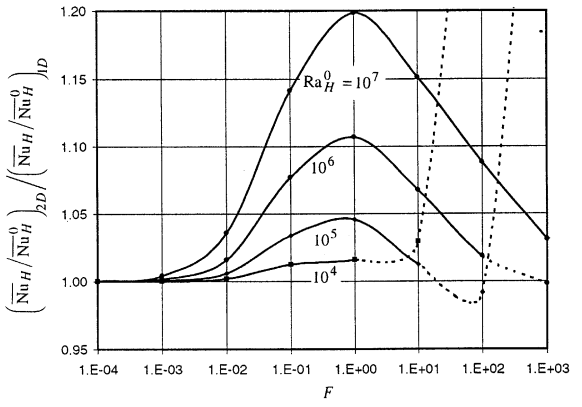

Fig. 5. The ratio $(\overline{Nu}_H/\overline{Nu}^0_H)_{2D}/(\overline{Nu}_H/\overline{Nu}^0_H)_{1D}$ as function of the F factor for some values of the Ra^0_H Rayleigh number.

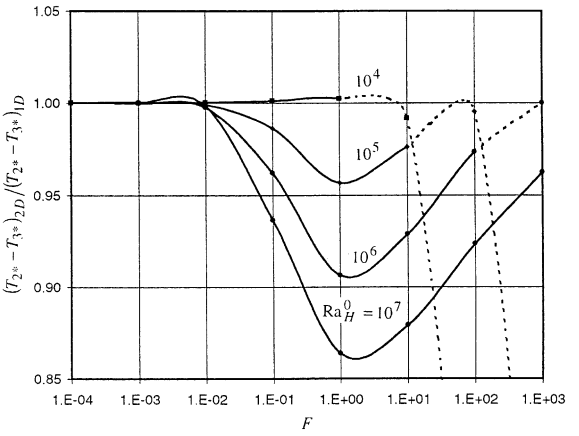

Fig. 6. The ratio $(T^*_2 - T^*_3)_{2D}/(T^*_2 - T^*_3)_{1D}$ as function of the F factor for some values of the Ra^0_H Rayleigh number.

values of Ra^0_H. Both correlation (1) and the 2D numerical simulation reproduces fairly well the $\overline{Nu}^0_H$ global Nusselt number for the enclosure without diffusive walls, the ratio under analysis being very close to the ratio $(\overline{Nu}_H)_{2D}/(\overline{Nu}_H)_{1D}$. One can conclude from this figure that the results are, as expected, very good and near unit for low values of the F factor. As Ra^0_H increases, the ratio also increases reaching its maximum for $F \approx 1$. It can be concluded that, in the worst case, always for $F \approx 1$, the effective Nusselt number obtained following the 1D approach is 83% of the reference value when $Ra^0_H = 10^7$, 90% when $Ra^0_H = 10^6$, 96% when $Ra^0_H = 10^5$, and 98% when $Ra^0_H = 10^4$. For $F > 1$, the ratio under analysis approaches the unit as F increases, for any of the considered Ra^0_H values. Over the considered domain, the effective Nusselt number obtained with the 1D approach, $(\overline{Nu}_H)_{1D}$, is under-estimated. It is also observed a very high value of the ratio under analysis when $F > 1$ for $Ra^0_H = 10^4$, when $F > 10$ for $Ra^0_H = 10^5$ and when $F > 100$ for $Ra^0_H = 10^6$. Such cases are represented by dashed lines in Fig. 5. This corresponds to specific cases where the Berkovsky and Polevikov correlation (1) is not valid, since they correspond to an effective Rayleigh number Ra_H less than the lower value admitted by the applicability conditions of the correlation. Thus, the very high values of the ratio under analysis are attributed to the use of correlation (1) out of its application domain, and are therefore non-valid results. It can also be observed that the 1D approach gives better results for lower values of Ra^0_H. Moreover, lower values of Ra^0_H lead more easily to lower values of the effective Rayleigh number Ra_H for which correlation (1) does not apply.

In Fig. 6 it is presented the ratio $(T_{2^*} - T_{3^*})_{2D}/(T_{2^*} - T_{3^*})_{1D}$ as function of the F factor for some values of Ra^0_H. In this case, a similar behavior to the one found for the effective Nusselt number can be observed. It has to be noted that the temperature difference obtained with the 1D procedure is in the majority of the cases over-estimated. In the worst case, also always for $F \approx 1$, the effective temperature difference obtained following the 1D approach is 116% of the reference value when $Ra^0_H = 10^7$, 110% when $Ra^0_H = 10^6$, 104% when $Ra^0_H = 10^5$, and 99% when $Ra^0_H = 10^4$. For $F > 1$, the ratio approaches the unit as F increases, for any of the considered Ra^0_H values. It is observed a very low value of the ratio under analysis when $F > 1$ for $Ra^0_H = 10^4$ and when $F > 10$ for $Ra^0_H = 10^5$, for the same reasons referred when analyzing Fig. 5, i.e. the existence of effective Rayleigh numbers Ra_H for which correlation (1) does not apply. Such situations are represented by dashed lines in Fig. 6.

In Fig. 7 it is presented the ratio $(\dot{Q}'/\dot{Q}'^0)_{2D}/(\dot{Q}'/\dot{Q}'^0)_{1D}$ as function of the F factor for different values

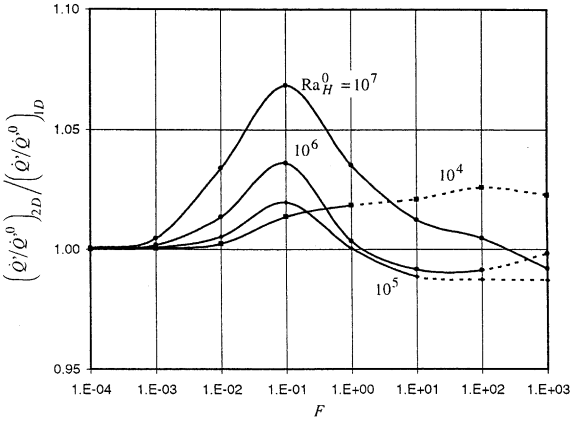

Fig. 7. The ratio $(\dot{Q}'/\dot{Q}'^0)_{2D}/(\dot{Q}'/\dot{Q}'^0)_{1D}$ as function of the F factor for some values of the Ra^0_H Rayleigh number.

of the Ra_H^0 Rayleigh number. Also here, correlation (1) and the 2D numerical modeling reproduce very well the $\overline{Nu}_H^0$ global Nusselt number for the enclosure without diffusive walls, thus leading to very good values of the heat flow by unit depth, and the ratio under analysis is very close to the ratio $(\dot{Q}')_{2D}/(\dot{Q}')_{1D}$. From a thermal engineering point of view, this might be the most relevant conclusion, since the main objective is the evaluation the heat effectively transferred through the complete enclosure with diffusive walls. The behavior of this ratio is similar to the one found for the effective Nusselt number. The effective heat transfer evaluated through the 1D approach is under-estimated for $F \leqslant 1$, for the Ra_H^0 Rayleigh numbers considered, and tends to be over-estimated for higher values of the F parameter and $Ra_H^0 \geqslant 10^5$. The worst cases for the heat transfer obtained following the 1D approach are always obtained when $F \approx 1$, being: 93% of the reference value when $Ra_H^0 = 10^7$, 97% when $Ra_H^0 = 10^6$, 98% when $Ra_H^0 = 10^5$, and 98% when $Ra_H^0 = 10^4$. In all the analyzed cases, it is observed a very good agreement between the results obtained with the 1D approach and the reference ones obtained from the complete 2D numerical simulation. As referred previously when analyzing Figs. 5 and 6, there are situations where the proposed 1D approach is not valid, presented by dashed lines in Fig. 7, due to the non-applicability of correlation (1) in such conditions.

The temperatures along the vertical surfaces $x_* = 0$ and $x_* = 1$ were assumed as constants in the 1D approach, and as average values in the post-processing of the results obtained with the 2D modeling (Eqs. (26)–(28)). Such assumption leads to a very good agreement between the 1D and 2D results, for both effective Nusselt number and effective heat flow transferred, proving itself valid for this specific purpose.

6. Conclusions

The results obtained following the proposed 1D approach are in very good agreement with those obtained with the complete 2D modeling. Taking the 2D results as the reference, the worst cases encountered in the analyzed situations present a deviation of 17% for the effective Nusselt number, a deviation of 10% for the effective temperature difference, and a deviation of 7% for the effective heat transfer. This 1D approach is also an effective way to enlarge the applicability domain of the usual correlations for the Nusselt number in rectangular enclosures to a situation for which such correlations were not obtained, i.e. for enclosures with diffusive walls.

Analyzed situations were restricted to a fluid with a Prandtl number of 0.73, and the comparison between the 1D and 2D results was restricted to a quadrangular enclosure. However, the 1D model could be extended also to rectangular enclosures and to other Prandtl number fluids, once guaranteed the applicability conditions of the available correlations for the Nusselt number. The Prandtl number is irrelevant to the 1D model, and the shape factor of the rectangular enclosures is also of minor relevance, once verified and tested the 1D model over the quadrangular enclosure and that the temperatures over the vertical solid–fluid interfaces are kept nearly constant.

The proposed 1D approach is thus an acceptable way to model the involved heat transfer through the complete enclosure. It proves to be a very useful tool to help the thermal engineer to correctly use the available correlations to obtain the effective Nusselt number and the effective heat transfer in real rectangular enclosures with diffusive vertical walls.

References

[1] A. Bejan, Convection Heat Transfer, second ed., Wiley, New York, 1995.
[2] G. de Vahl Davis, Natural convection of air in a square cavity: A bench mark numerical solution, Int. J. Numer. Meth. Fluids 3 (1983) 249–264.
[3] I. Catton, Natural convection in enclosures, in: Proceedings of the 6th International Heat Transfer Conference vol. 6, Toronto, Canada, 1978, pp. 13–43.
[4] T. Nishimura, F. Nagasawa, Y. Kawamura, Natural convection in horizontal enclosures with multiple partitions, Int. J. Heat Mass Transfer 32 (9) (1989) 1641–1647.
[5] V.A.F. Costa, Double diffusive natural convection in a square enclosure with heat and mass diffusive walls, Int. J. Heat Mass Transfer 40 (17) (1997) 4061–4071.
[6] F. Alavyoon, On natural convection in vertical porous enclosures due to prescribed fluxes of heat and mass at the vertical boundaries, Int. J. Heat Mass Transfer 36 (10) (1993) 2479–2498.
[7] D.M. Kim, R. Viskanta, Effect of wall heat conduction on natural convection heat transfer in a square enclosure, ASME J. Heat Transfer 107 (1985) 139–146.
[8] Z.-G. Du, E. Bilgen, Coupling of wall conduction with natural convection in a rectangular enclosure, Int. J. Heat Mass Transfer 35 (8) (1992) 1969–1975.
[9] C.J. Ho, Y.H. Lin, Thermal convection heat transfer of air/water layers enclosed in horizontal annuli with mixed boundary conditions, Wärme-und Stoffübertragung 24 (1989) 211–224.
[10] C.J. Ho, Y.H. Lin, T.C. Chen, A numerical study of natural convection in concentric and eccentric horizontal cylindrical annuli with mixed boundary conditions, Int. J. Heat Fluid Flow 10 (1989) 40–47.
[11] C.J. Ho, Y.H. Lin, Natural convection of cold water in a vertical annulus with constant heat flux on the inner wall, ASME J. Heat Transfer 112 (1990) 117–123.

[12] V.A.F. Costa, Double diffusive natural convection in enclosures with heat and mass diffusive walls, in: G. De Vahl Davis, E. Leonardi (Eds.), Proceedings of the International Symposium on Advances in Computational Heat Transfer (CHT'97), Begell House, New York, 1998, pp. 338–344.
[13] V.A.F. Costa, Convecção natural induzida por diferenças de temperatura e de concentração numa cavidade quadrangular com paredes difusivas, in: Proceedings of the III Congreso Iberoamericano de Ingeniería Mecánica (CIDIM'97), (CD edited), Habana, Cuba, 1997, work 2–275.
[14] S.V. Patankar, Numerical Heat Transfer and Fluid Flow, Hemisphere/McGraw-Hill, Washington, DC, 1980.
[15] V.A.F. Costa, Unification of the streamline, heatline and massline methods for the visualization of two-dimensional transport phenomena, Int. J. Heat Mass Transfer 42 (1) (1999) 27–33.